Volume 6, Number 3 ACTA PHYSICA SINICA March,1997
1004-423X/97/06030189-08 (Overseas Edition) ©1997 Chin.Phys.Soc.

A THEORETICAL SIMULATION FOR ACHIEVING HIGH SPATIAL COHERENCE OF LABORATORY X-RAY LASERS*

LI JING-HONG(李敬宏), PENG HUI-MIN(彭惠民), ZHANG GUO-PING(张国平), and YANG MING-LUN(杨明伦)

Institute of Applied Physics and Computational Mathematics, Beijing 100088, *China*

(Received 4 July 1996)

An efficient method to achieve high spatial coherence of laboratory soft-X-ray laser is presented, in which a pinhole can be used in "four-target series coupling" experiment to obtain a fully coherent X-ray laser. The model of amplified spontaneous emission is used to describe the characteristics and spatial coherence properties of a soft-X-ray laser beam. The simulation results show that the method is feasible.

PACC: 4255V

I. INTRODUCTION

The rapid development of laboratory soft-X-ray lasers and the intent to use X-ray laser in holography have stimulated much interest in their coherence properties. The longitudinal coherence based on the measured and estimated intrinsic linewidths appears sufficient, but spatial coherence remains problematic. Theoretical study of the spatial coherence of the laser field requires to solve a wave equation. There are at present two main analytic approaches for understanding X-ray laser spatial coherence: 1.Modal method: The electric field is written as a mode expansion, and the paraxial wave equation is transformed into a transverse eigenvalue-eigenfunction ("mode") equation. By solving the mode equation, one can study the coherence.[1−3] 2.Wave-optics propagation method: Using the model of amplified spontaneous emission (ASE) based on an electric field driven by random noise, one obtains the output field of X-ray laser by numerically solving the paraxial wave equation.[4,5] There were also some experiments to measure the spatial coherence of laboratory X-ray laser.[6,7]

*Project supported by the Fund for Young Scientists in the Laser Domain of the Chinese National High Technology Plan.

The previous studies showed that good spatial coherence appeared to be more difficult to achieve.

This paper presents an efficient method to obtain high spatial coherence of laboratory soft-X-ray laser, in which a pinhole can be used in "four-target series coupling" experiment[8] to obtain a fully coherent X-ray laser. The model of ASE is used to describe the output beam characteristics and spatial coherence properties of laboratory soft-X-ray laser. The simulation results show that this method is feasible.

This paper is organized as follows: In section 2 we present the scheme for achieving high spatial coherence. The ASE model is described in section 3. Section 4 contains the numerical results, and a summary is presented in section 5.

II. A SCHEME FOR ACHIEVING HIGH SPATIAL COHERENCE

With the electron collisional excitation mechanism in laboratory soft-X-ray laser, using long duration pulse pump laser to irradiate the thick target, we can obtain a good plasma gain region: 1. the width of the gain region is greater than 100 μm; 2. the lasing duration is long, about several hundreds of nanoseconds; 3. during lasing, the plasma state and the position of gain region are maintained unchanged on the whole. These favourable conditions are suitable for achieving high spatial coherence of laboratory soft-X-ray laser.

Based on the above idea, experiments of "Double-Target Opposing Coupling" [11] and "Multi-Target Series Coupling"[8,14,15] have been carried out successfully in China, and deep saturation of gain was reached.

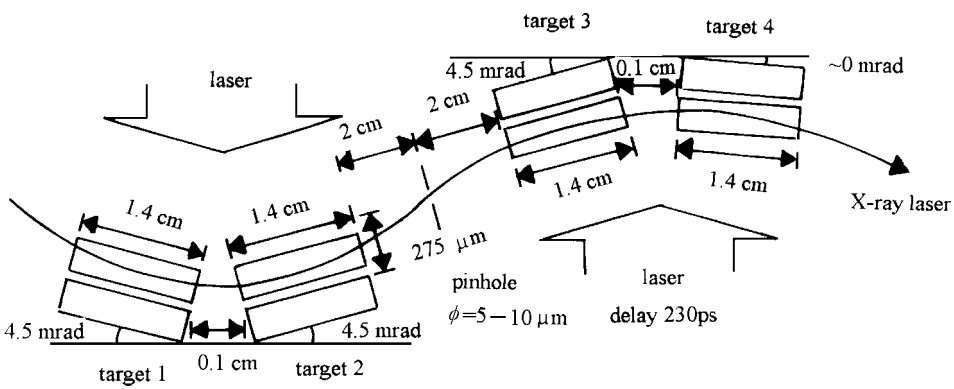

Fig. 1. Schematic diagram for achieving high spatial coherence of the laboratory soft-X-ray laser.

Figure 1 is a schematic diagram for achieving high spatial coherence of laboratory soft-X-ray laser, which is based on the "four-target series coupling" experiment carried out in China.[8] A similar scheme was proposed in an early time[9], in which a fully coherent source with a diameter of 25 μm is needed to drive an amplifier. The difficulty is how to construct the source. In our scheme, the first two targets and a pinhole are used as the X-ray laser

source, and the other two targets are used as amplifiers. The spatial coherence of X-ray laser from the first two targets is so poor that the spatial coherent length of the beam is only about several microns. In order to match it, a pinhole with a diameter of about several microns is used to get an output with high spatial coherence. The pinhole should be kept some distance away from target 2 and target 3 in order to avoid being damaged by the plasma.

III. MODEL FOR ASE

Analogous to Ref. [4], as the starting point, we describe an ASE based on the paraxial equations for slowly varying wave electric-field, in which the diffraction, gain saturation, and refractive effects due to electron density gradients are included. The equation describing the counterpropagating beams is

$$E = E^{+}\exp[\mathrm{i}(kz - \omega t)] + E^{-}\exp[\mathrm{i}(kz + \omega t)], \tag{1}$$

where the complex fields amplitudes, E^{+} and E^{-}, satisfy the paraxial wave equations

$$2\mathrm{i}k\left(\frac{n}{c}\frac{\partial E^{\pm}}{\partial t} \pm \frac{\partial E^{\pm}}{\partial z}\right) = \bigtriangledown_{\perp}^{2}E^{\pm} + k^{2}(n^{2}-1)E^{\pm} + \mathrm{i}gkE^{\pm} + \mathrm{i}kS^{\pm}(x,z). \tag{2}$$

Here $\bigtriangledown_{\perp}^{2} = \frac{\partial^{2}}{\partial x^{2}} + \frac{\partial^{2}}{\partial y^{2}}$, g is a saturable gain coefficient, $k = \omega/c$, n is the refractive index,and $S^{\pm}$ are stochastic sources defined by

$$S^{\pm}(x,y,z,t) = A(x,y,z,t)\exp[\mathrm{i}2\pi\Phi^{\pm}(x,y,z,t)], \tag{3}$$

where random phases $\Phi^{\pm}(x,y,z,t)$ are evaluated from pseudorandom numbers. The saturable gain coefficient has the form

$$g = \frac{g_{0}}{1 + I/I_{\mathrm{sat}}}, \quad I = \mid E^{+} \mid^{2} + \mid E^{-} \mid^{2}, \tag{4}$$

where g_{0} is the small-signal gain coefficient,and the saturation intensity is given by

$$I_{\mathrm{sat}} = \frac{8\pi h\nu^{3}}{c^{2}}\left(\frac{1}{\tau A_{\mathrm{ul}}}\right)\Delta\nu_{0}. \tag{5}$$

Here $\Delta\nu_{0}$ represents the atomic linewidth, ν is the frequency of X-ray laser, τ is the total lifetime of the upper level of laser, and A_{ul} is the spontaneous emission coefficient from upper to lower laser level. The spontaneous emission normalization constant A in Eq.(3) can be determined from the laser transition rate equations and the transfer equation governing the laser radiation. The result is

$$A = \frac{2g^{1/2}}{(\Delta z)^{1/2}}\left(I_{\mathrm{sat}}\frac{\Delta\nu_{L}}{\Delta\nu_{0}}\frac{\Delta\Omega}{4\pi}\right)^{1/2}, \tag{6}$$

where $\Delta\nu_L$ is the frequency bandwidth of the laser radiation, Δz is the step along the z axis, and $\Delta\Omega \approx \pi(\Delta\theta)^2$ is the solid angle, here $\Delta\theta$ is the beam divergence, and $\Delta\nu_L/\Delta\nu_0$=1 is assumed. Equation (2) is solved by using the fast-Fourier-transform-based split-operator algorithm.[10]

In the calculation, the output intensity of the X-ray laser from a single target is much less than the saturation intensity, so that only the electric field E^+ along the positive z axis is considered. The coupling of laser between two targets can be solved by using the following method: First the propagation is calculated, and then the laser beam is adjusted by the angle made between the two targets.

IV. NUMERICAL RESULTS

The ASE model has been applied to the Ne-like Ge X-ray laser, and compared with the "multi-target series coupling" experiments.[8,11] The numerical results agreed with the experiments very well.[12] In this paper, the typical parameters are listed below: The wavelength of X-ray laser is 23.2 nm. Like the "four-target series coupling" experiment, the plasma length of every target is 1.4 cm; the pump laser has a wavelength of 1.05 μm; the temporal full width at half maximum of the pulse with a Gaussian shape is about 1 ns. An energy about 600 J is focused onto the thick Ge slabs, and the laser power density in the focused line is 1×10^{13} W/cm^2. Separation between target 2 and target 3 is 4 cm, and the gap between the surface planes of target 2 and target 3 is 550 μm. A pinhole with a diameter of 10 μm is placed at the center of the gap between targets 2 and 3, and 275 μm above the surface plane of target 2. It is difficult to grasp the temporal history of X-ray laser spatial coherence in our theoretical simulation, because we need high-precision temporal and spatial distributions of the plasma, so we only study the time- independent behavior of X-ray laser. The spatial distributions of electron density and gain coefficient of plasma are provided by JB19[13] and ALPHA codes. In our computation, we take the peak of pump laser to be at 1.29 ns, the plasma states of targets 1 and 3 at 1.39 ns and targets 2 and 4 at 1.45 ns. The laser is represented on a rectangular grid with 4096 divisions in transverse direction and 200 divisions in the longitudinal direction. The beam divergence angle is chosen to be 10 mrad, the spatial extent of the grid in transverse direction is 1000 μm, and the calculated results are averaged every 50 cycles.

The complex degree of coherence of the field at two points x_0 and x is given by

$$\mu(x) = \frac{< E^*(x_0,t)E(x,t) >}{\left[<\mid E(x_0,t) \mid^2><\mid E(x,t) \mid^2> \right]^{1/2}}, \tag{7}$$

where the angular bracket $< >$ denotes a time average. When the laser is nonstationary, the angular bracket $< >$ should really denote an ensemble average. The spatial coherence is characterized by the absolute value of the complex degree of coherence. According to the

criterion $|\mu(x)|$=0.88, we can calculate the spatial coherence length.

We compare the spatial coherences for three cases: 1.with no pinhole; 2.with a pinhole 5 μm in diameter; and 3.with a pinhole 10 μm in diameter. The spatial intensity (near-field) distributions, the spatial coherence, and the angular intensity (far-field) distributions of X-ray laser through every target are shown in Fig.2 for the setup without a pinhole and Fig.3 for that with a pinhole. During the computation, we choose the point x_0 near the peak point in the spatial intensity distribution, then calculate the spatial coherences at two points x_0 and x as functions of x. Figure 2 shows that the spatial coherence length increases with the

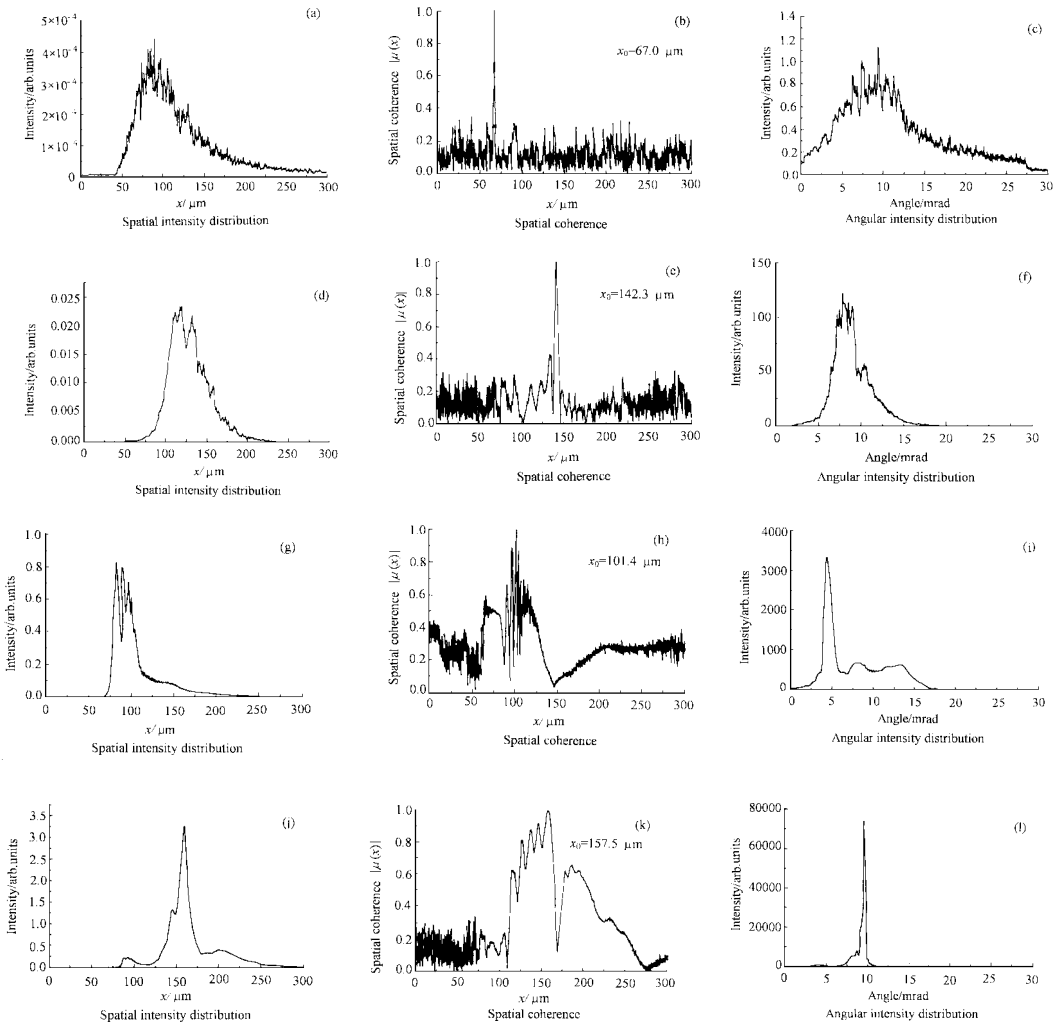

Fig.2. X-ray laser intensity distributions and spatial coherence without a pinhole.(a)–(c) outputs through target 1, (d)–(f) outputs through target 2, (g)–(i) outputs through target 3, (j)–(l) outputs through target 4.

number of target (or plasma length), while spatial coherence length is still very short. If a pinhole is placed in the setup, then the spatial coherence of the output fields through the last two targets is improved greatly, as shown in Fig.3. Figures 3(a)–3(c) show the outputs through target 3 with a pinhole diameter of 10 μm, Figs.3(d)–3(f) show the outputs through target 3 with a pinhole diameter of 5 μm, Figs.3(g)–3(i) show the outputs through target 4 with a pinhole diameter of 10 μm, and Figs.3(j)–3(l) show the outputs through target 4 with a pinhole diameter of 5 μm. In Fig.3 the spatial coherence lengths of the final outputs for the pinholes with diameters of 5 and 10 μm are greater than 100 μm, and the spatial

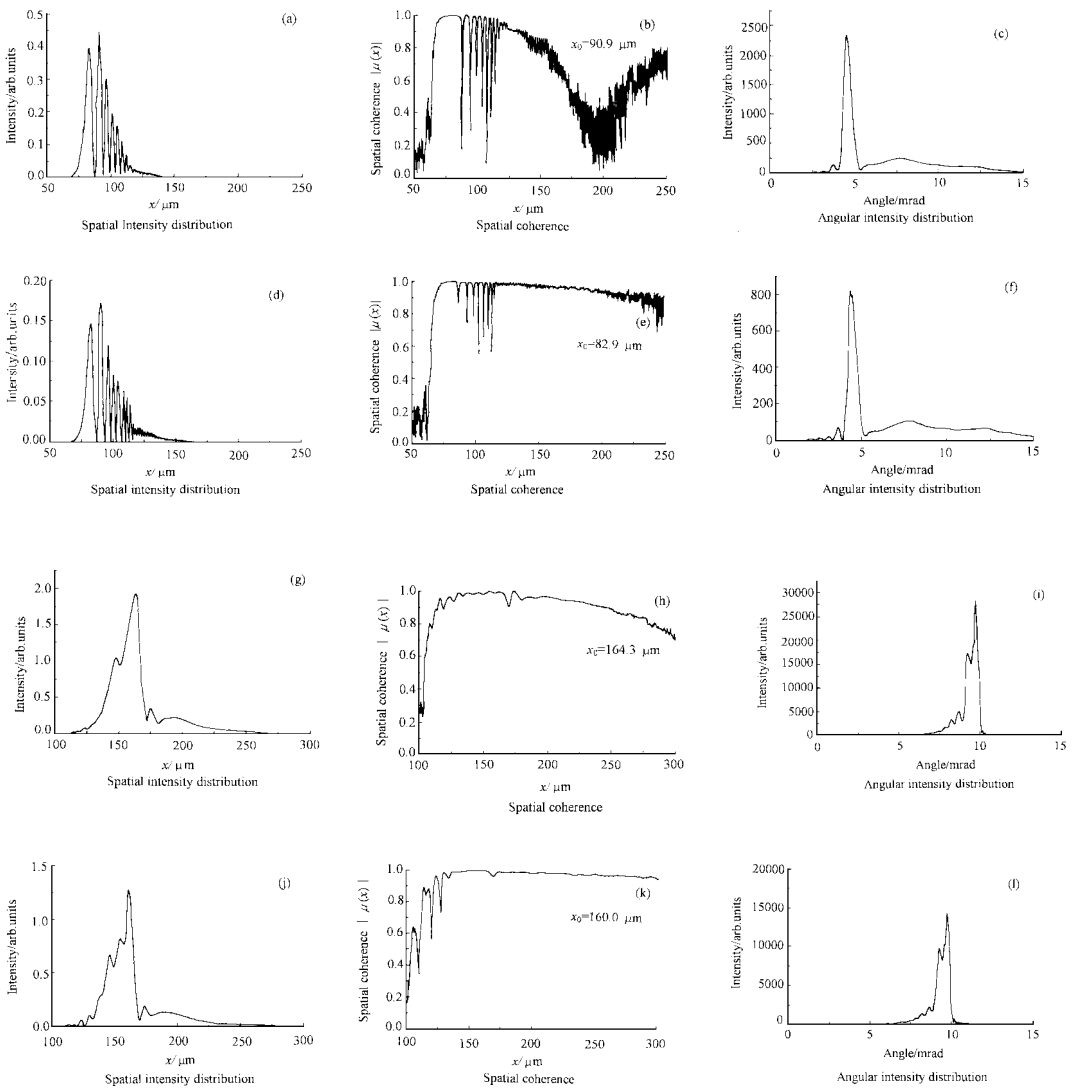

Fig.3. X-ray laser intensity distributions and spatial coherence with a pinhole.(a)–(c) outputs through target 3, pinhole diameter 10 μm, (d)–(f) outputs through target 3, pinhole diameter 5 μm, (g)–(i) outputs through target 4, pinhole diameter 10 μm, (j)–(l) outputs through target 4, pinhole diameter 5 μm.

coherence length for a pinhole diameter of 5 μm is longer than that for a pinhole diameter of 10 μm.

Our simulation results also show that the location of the pinhole from the surface plane of target 2 can vary in a wide range due to the wide spatial intensity distribution of X-ray laser at the pinhole plane. Both Fig.3(g) and Fig.3(j) show that the peak intensities of X-ray lasers in the spatial intensity distribution are higher than the saturation intensity, and not much lower than that in the setup without a pinhole. Both Fig.3(i) and Fig.3(l) show that the beam divergence of X-ray laser are about 2 mrad (full-width at half-maximum). So this X-ray laser meets the need of X-ray laser holography in the brightness, the longitudinal and spatial coherences. We can use this X-ray laser for taking holography.

V. SUMMARY

A scheme for achieving high spatial coherent X-ray laser is proposed in this paper, in which a pinhole can be used in "four-target series coupling" experiment to obtain a fully coherent X-ray laser. The numerical results show that the spatial coherence of the output of X-ray laser is good enough to be used for the demonstration of X-ray laser holography. In practical application, the single lasing line, such as the 19.6 nm line of the Ne-like Ge X-ray laser, should be used as X-ray laser source. With the improvement of X-ray laser and X-ray optics, it is believed that biological holography will come true in the near future.

REFERENCES

[1] R. A. London, M. Strauss and M. D. Rosen, *Phys. Rev. Lett.*, **65**(1990), 563.

[2] P. Amendt and R. A. London, *Phys. Rev.*, **A44**(1991), 7478.

[3] P. Amendt, R. A. London and M. Strauss, *Phys. Rev.*, **A47**(1993), 4348.

[4] M. D. Feit and J. A. Fleck, Jr., *J. Opt. Soc. Am.*, **B7**(1990), 2048.

[5] M. D. Feit and J. A. Fleck, Jr., *Opt. Lett.*, **16**(1991), 76.

[6] J. E. Trebes, K. A. Nugent, S. Mrowka, R. A. London, T. W. Barbee, M. R. Carter, J. A. Koch, B. J. MacGowan, D. L. Matthews, L. B. Da Silva, G. F. Stone and M. D. Feit, *Phys. Rev. Lett.*,**68**(1992), 588.

[7] R. E. Burge, G. E. Slark, X. Cheng, M. T. Browne, D. Neely, C. L. S. Lewis and A. MacPhee, *Proc. SPIE*, **2520**(1995), 257.

[8] Wang Shiji, Gu Yuan, Zhou Guanlin, Ni Yuanlong, Yu Songyu, Fu Sizu, Mao Chusheng, Tao Zucong, Chen Wannian, Lin Zunqi, Fan Dianyuan, Zhang Guoping, Sheng Jiatian, Yang Minglun, Zhang Tanxin, Shao Yunfeng, Peng Huimin, He Xiantu and Yu Min, *Chin. Phys. Lett.*, **8**(1991), 618.

[9] M. D. Rosen, J. E. Trebes and D. L.Matthews, *Comments Plasma Phys. Controlled Fusion*, **10**(1987),245.

[10] J. W. Greene, *Phys. Rev.*, **E48**(1993), 3130.

[11] Wang Shiji, Gu Yuan, Fu Sizu, Zhou Guanlin, Yu Songyu, Ni Yuanlong, Wu Jiang, Han Guoqiang, Zhou Zhengliang, Wan Binggen, Tao Zucong, Peng Huimin, Sheng Jiatian, Zhang Tanxin, Shao Yunfeng, Zhang Guoping, Lin Zunqi, Wang Shushen, Chen Wannian and Fan Dianyuan, *Science in China (Series A)*, **2**(1991), 151 (in Chinese).

[12] Li Jinghong, Zhang Guoping, Peng Huimin and Yang Minglun, *Acta Optica Sinica*, **16**(1996), 1356 (in Chinese).

[13] Zhang Guoping, Sheng Jiatian, Peng Huimin and Shao Yunfeng, *High Power Laser and Particle Beams*, **2**(1990), 298 (in Chinese).

[14] Shiji Wang, Yuan Gu, Chusheng Mao, Zhengliang Zhou, Guanlin Zhou, Yuanlong Ni, Songyu Yu, Yuenan Xiong, Binggen Wan, Weibuo Ji, Sizu Fu, Guoqiang Han, Guanlong Huang, Dianyuan Fan, Zunqi Lin and Ximing Deng, *Chin. J. Laser*, **B2**(1993), 481.

[15] Wang Shiji, Gu Yuan, Zhou Guanlin, Zhou Zhengliang, Ni Yuanlong, Yu Songyu, Fu Sizu, Mao Chusheng, Han Guoqiang, Wan Binggen, Ji Weibo, Wu Jiang, Zeng Yixin, Chen Wannian and Huang Guanlong, *High Power Laser and Particle Beams*, **5**(1993), 557 (in Chinese).